# RADIATION-INDUCED POWER DEGRADATION FOR GaAs/Ge SOLAR ARRAYS

Thomas W. Woike
Applied Solar Energy Corporation
City of Industry, CA 91749

## Abstract

This paper presents new radiation-induced power degradation data for GaAs/Ge solar arrays applicable to missions ranging from low earth orbit (LEO) to geosynchronous earth orbit (GEO) and compares these results to silicon arrays. These results are based on recently published radiation damage coefficients for GaAs/Ge cells. The power density ratio (GaAs/Ge to Si BSF/R) has been found to be as high as 1.83 for the proton-dominated worst-case altitude of 7408 km (MEO). Based on the EOL GaAs/Ge solar array power density results for MEO, missions which were previously considered infeasible may be reviewed based on these more favorable results. The additional life afforded by using GaAs/Ge cells is an important factor in system-level trade studies when selecting a solar cell technolgy for a mission and needs to be considered. The data presented in this paper is expected to support this decision since the selected orbits have characteristics similar to most orbits of interest.

## I. Introduction

EOL power estimates for solar array designs are significantly influenced by the predicted degradation due to charged-particle radiation. This paper presents new radiation-induced power degradation data for GaAs/Ge cells applicable to missions ranging from low earth orbit (LEO) to geosynchronous earth orbit (GEO) and compares these results to silicon arrays. These results are based on recently published radiation damage coefficients for GaAs/Ge cells[1].

Since the 1980s, production quantities of GaAs solar cells have been available. Within the last few years, MOCVD growth of high-quality GaAs films on Ge substrates has enabled these high-efficiency cells to be manufactured in large volume at a lower cost.

GaAs/Ge solar cells have significant advantages over silicon cells for space-based solar arrays:

> The efficiency (BOL, AM0, 28°C) of space-qualified, production-grade, MOCVD-grown GaAs/Ge cells is greater than 18%, compared to less than 15% for conventional silicon cells and less than 16% for textured silicon cells.
>
> The Pmax temperature coefficient for GaAs/Ge is more favorable than the value for silicon.
>
> For almost all missions, GaAs/Ge cells are more resistant to radiation-induced power degradation than silicon cells.

This degradation is typically established by first converting the proton and electron spectra associated with an orbit to an equivalent fluence of 1 MeV electrons and then assigning a degradation value based on 1 MeV electron radiation data for the cell type of interest. This methodology is used to determine the radiation-induced power degradation results presented in this paper.

## II. Analysis Description

Thirteen orbits of general interest were selected for this study. These orbits were chosen to provide results across the broadest spectrum possible:

Low Earth Orbit (LEO)
Altitude 926 km (500 n.mi.)
Inclinations 0°,30°,60°,90°

Medium Earth Orbit (MEO)
Altitude 7408 km (4000 n.mi.)
Inclinations 0°,30°,60°,90°

High Earth Orbit (HEO)
Altitude 20372 km (11000 n.mi.)
Inclinations 0°,30°,60°,90°

Geosynchronous Earth Orbit (GEO)
Altitude 35794 km (19327 n.mi.)
Inclination 0°

Equivalent annual 1 MeV electron fluences for these orbits were determined[2] by multiplying the electron and proton spectra for these orbits and the damage coefficients established for the solar cell material, and converting the proton results to equivalent 1 MeV electrons. This was done for both Si BSF/R and GaAs/Ge solar cells. The AEI7LO and AP8MAX radiation models were used for electrons and protons respectively. Six fluences were determined for each orbit, representing 3, 6, 12, 20, 30, and 60 mil coverglass thicknesses.

These equivalent annual fluences were then used to determine total mission equivalent fluence for mission lengths from 0.5 to 10 years. Based on these total exposures, power degradation factors were then determined from published degradation characteristics for GaAs/Ge[1] and Si BSF/R[3] solar cells.

These degradation factors were then applied to BOL power densities for GaAs/Ge and Si BSF/R solar arrays to determine the EOL power density characteristics presented in Section III.

The BOL power densities were established by assuming AM0 illumination at normal incidence, 100% packing factor, no assembly losses, no environmental losses except for radiation degradation, and infinite backshielding for both array types. Even though some of these characteristics may not be achievable in practice, these assumptions allow for simpler analysis without invalidating the GaAs/Ge and Si BSF/R comparison. Operating temperature is assumed to be 55°C and 50°C for GaAs/Ge and Si BSF/R cells respectively, while their BOL AM0 28°C efficiencies are assumed to be 18.3% and 14.7%.

Finally solar flare protons are assumed to be negligible. This assumption holds for LEO and MEO. In HEO and GEO, solar flare protons comprise about 10% - 30% of total equivalent fluence. Since GaAs/Ge cells are more resistant to protons (as reported in the next section) than Si BSF/R cells, the inclusion of solar flare protons would improve the relative performance of GaAs/Ge cells beyond the results reported in this paper.

## III. Results

### Annual Equivalent Fluence Data

Tables 1 - 4 show that the annual equivalent fluences for GaAs/Ge and Si BSF/R arrays are about the same for the electron-dominated HEO and GEO orbits, while Si BSF/R is subjected to about a factor of 3 higher equivalent fluence than GaAs/Ge in the proton-dominated LEO and MEO orbits.

### Low Earth Orbit (LEO) Power Predictions 926 km (500 n.mi.)

As shown in Figures 1 - 4, the GaAs/Ge solar array power density is greater than 216 W/m$^2$ for a ten year design life using a 3 mil or thicker coverglass over all inclinations studied at the chosen altitude of 926 km (500 n.mi.). Figures 5 - 8 demonstrate that the EOL power advantage of GaAs/Ge over Si BSF/R increases with increasing mission duration and decreasing coverglass thickness, with 60° being approximately the optimum inclination. For a ten year design life, GaAs/Ge provides between 48% to 70% higher EOL power than Si BSF/R when a 3 mil coverglass is used. This range is 48% to 62% for a 6 mil coverglass.

Medium Earth Orbit (MEO) Power Predictions
7408 km (4000 n.mi.)

Figure 9 shows that even at this nearly worst-case radiation altitude, the GaAs/Ge solar array power density exceeds 180 $W/m^2$ after five years at the worst-case inclination of 0°, provided that a 60 mil coverglass is used. The 180 $W/m^2$ value serves as an important benchmark because this slightly exceeds the BOL Si BSF/R solar array power density. Figure 10 indicates that for 30° inclination the GaAs/Ge solar array power density will not degrade to the BOL Si BSF/R solar array power density value until 3.5 years when a thinner 30 mil coverglass is used. Figure 11 shows that the same can be said at 60° inclination after 1.9 and 6.5 years when using a 20 mil and 30 mil coverglass respectively. Figure 12 demonstrates that a polar orbit (90° inclination) improves the aforementioned values to 2.1 and 7.5 years.

As evidenced by Figures 13 - 16, the comparison between GaAs/Ge and Si BSF/R solar array power density is incomplete for this altitude. Since the highest radiation exposure on JPL's test cells is $10^{16}$ 1 MeV electrons/$cm^2$, no EOL power densities are calculated when total mission fluence exceeds this value. Notwithstanding, the use of GaAs/Ge is particularly beneficial at this altitude since EOL power densities as high as 83% above those of Si BSF/R can be attained.

High Earth Orbit (HEO) Power Predictions
20372 km (11000 n.mi.)

Figures 17 - 20 demonstrate that at this altitude the GaAs/Ge solar array power density after nine years of life exceeds the BOL Si BSF/R solar array power density value for all inclinations studied when a standard 6 mil coverglass is used. Figures 21 - 24 indicate that the EOL GaAs/Ge solar array power density is generally at least 50% higher than for Si BSF/R for most design lifes.

Geosynchronous Earth Orbit (GEO) Power Predictions
35794 km (19327 n.mi.)

Figure 25 shows that in GEO the GaAs/Ge solar array power density after ten years of life is about 210 $W/m^2$ (6 mil coverglass) compared to the BOL Si BSF/R solar array power density of almost 180 $W/m^2$ . Figure 26 demonstrates that throughout the design life, GaAs/Ge typically affords a 40% to 50% power density improvement over Si BSF/R .

## IV. Conclusions

Recently published damage coefficients for GaAs/Ge solar cells and updated normalized power degradation characteristics[1] were used to predict EOL power for 13 selected orbits of general interest.

The equivalent fluences[2] for GaAs/Ge and Si BSF/R arrays are about the same for the electron-dominated HEO and GEO orbits, while Si BSF/R is subjected to about a factor of 3 higher equivalent fluence than GaAs/Ge in the proton-dominated LEO and MEO orbits.

At the beginning of life (BOL), the GaAs/Ge solar array power density is about 240 $W/m^2$ , compared to nearly 180 $W/m^2$ for Si BSF/R . This 33% advantage is entirely due to higher initial efficiency (18.3% versus 14.7%) and a more favorable temperature coefficient. This power density ratio then initially increases with mission life. In all but 16 of the 78 cases studied, the power density ratio continues to increase out to a ten year design life. For the other cases, the ratio peaks and then decreases slightly, but never below 1.5 (50% EOL power advantage for GaAs/Ge).

The power density ratio has been found to be as high as 1.83 for the proton-dominated worst-case altitude of 7408 km (MEO). Based on the EOL GaAs/Ge solar array power density results for MEO, missions which were previously considered infeasible may be reviewed based on these more favorable results.

The additional life afforded by using GaAs/Ge is an important factor in system-level trade studies when selecting a solar cell technolgy for a mission and needs to be considered. The higher EOL/BOL power ratio of a GaAs/Ge array translates into more relaxed requirements for power conditioning equipment and reduces the need for dissipative components to remove the additional BOL power for an array designed for EOL operation, thereby reducing system costs. The advantage in operating life also supports a favorable EOL power to weight ratio for a GaAs/Ge array.


## Acknowledgement

Special thanks to B. Anspaugh of JPL for providing the equivalent fluence data for the selected orbits based on the new GaAs/Ge damage coefficients.


## References


1. B. Anspaugh, "Proton and Electron Damage Coefficients for GaAs/Ge Solar Cells," 22nd IEEE Photovoltaic Specialists Conference, p.1593, 1991.

2. B. Anspaugh, Private Communication.

3. B. Anspaugh, "Solar Cell Radiation Handbook, Addendum 1: 1982-1988," JPL Publication 82-69, Addendum 1, 1989.

Table 1
Total Annual Pmax Equivalent Fluence for 0° Inclination

| Total Annual Fluence for Pmax<br>1 MeV equivalent electrons/cm^2<br><br>0° Inclination | | | | | | |
|---|---|---|---|---|---|---|
| Altitude (km) | Coverglass thickness (mils) | | | | | |
| | 3 | 6 | 12 | 20 | 30 | 60 |
| | GaAs/Ge | | | | | |
| 926 | 2.05e+12 | 1.93e+12 | 1.79e+12 | 1.67e+12 | 1.54e+12 | 1.38e+12 |
| 7408 | 1.39e+17 | 4.50e+16 | 9.46e+15 | 3.32e+15 | 9.38e+14 | 2.32e+14 |
| 20372 | 1.82e+14 | 1.41e+14 | 1.14e+14 | 8.97e+13 | 6.88e+13 | 3.36e+13 |
| 35794 | 3.12e+13 | 2.49e+13 | 1.73e+13 | 1.16e+13 | 7.47e+12 | 2.38e+12 |
| | Si BSF/R | | | | | |
| 926 | 5.86e+12 | 5.48e+12 | 4.99e+12 | 4.48e+12 | 4.14e+12 | 3.61e+12 |
| 7408 | 4.12e+17 | 1.47e+17 | 3.52e+16 | 1.03e+16 | 3.96e+15 | 8.21e+14 |
| 20372 | 2.08e+14 | 1.61e+14 | 1.29e+14 | 1.01e+14 | 7.75e+13 | 3.78e+13 |
| 35794 | 3.10e+13 | 2.48e+13 | 1.72e+13 | 1.15e+13 | 7.36e+12 | 2.34e+12 |

Table 2
Total Annual Pmax Equivalent Fluence for 30° Inclination

| Total Annual Fluence for Pmax<br>1 MeV equivalent electrons/cm^2<br><br>30° Inclination | | | | | | |
|---|---|---|---|---|---|---|
| Altitude (km) | Coverglass thickness (mils) | | | | | |
| | 3 | 6 | 12 | 20 | 30 | 60 |
| | GaAs/Ge | | | | | |
| 926 | 1.09e+13 | 9.23e+12 | 7.52e+12 | 6.31e+12 | 5.22e+12 | 4.20e+12 |
| 7408 | 6.11e+16 | 1.85e+16 | 3.66e+15 | 1.28e+15 | 3.61e+14 | 9.00e+13 |
| 20372 | 1.18e+14 | 9.51e+13 | 7.62e+13 | 5.94e+13 | 4.50e+13 | 2.13e+13 |
| | Si BSF/R | | | | | |
| 926 | 3.50e+13 | 2.97e+13 | 2.38e+13 | 1.87e+13 | 1.58e+13 | 1.19e+13 |
| 7408 | 1.77e+17 | 5.99e+16 | 1.36e+16 | 3.95e+15 | 1.51e+15 | 3.16e+14 |
| 20372 | 1.33e+14 | 1.06e+14 | 8.52e+13 | 6.62e+13 | 4.99e+13 | 2.36e+13 |

Table 3
Total Annual Pmax Equivalent Fluence for 60° Inclination

Total Annual Fluence for Pmax
1 MeV equivalent electrons/cm^2

60° Inclination

| Altitude (km) | Coverglass thickness (mils) | | | | | |
|---|---|---|---|---|---|---|
| | 3 | 6 | 12 | 20 | 30 | 60 |
| | GaAs/Ge | | | | | |
| 926 | 1.72e+13 | 9.56e+12 | 5.60e+12 | 4.14e+12 | 3.10e+12 | 2.29e+12 |
| 7408 | 3.13e+16 | 9.60e+15 | 1.92e+15 | 6.75e+14 | 1.92e+14 | 4.86e+13 |
| 20372 | 5.97e+13 | 4.71e+13 | 3.76e+13 | 2.93e+13 | 2.21e+13 | 1.04e+13 |
| | Si BSF/R | | | | | |
| 926 | 5.35e+13 | 3.13e+13 | 1.82e+13 | 1.21e+13 | 9.37e+12 | 6.51e+12 |
| 7408 | 9.10e+16 | 3.10e+16 | 7.13e+15 | 2.08e+15 | 7.98e+14 | 1.66e+14 |
| 20372 | 6.78e+13 | 5.28e+13 | 4.20e+13 | 3.26e+13 | 2.45e+13 | 1.16e+13 |

Table 4
Total Annual Pmax Equivalent Fluence for 90° Inclination

Total Annual Fluence for Pmax
1 MeV equivalent electrons/cm^2

90° Inclination

| Altitude (km) | Coverglass thickness (mils) | | | | | |
|---|---|---|---|---|---|---|
| | 3 | 6 | 12 | 20 | 30 | 60 |
| | GaAs/Ge | | | | | |
| 926 | 1.25e+13 | 7.17e+12 | 4.34e+12 | 3.27e+12 | 2.50e+12 | 1.86e+12 |
| 7408 | 2.70e+16 | 8.27e+15 | 1.66e+15 | 5.81e+14 | 1.65e+14 | 4.15e+13 |
| 20372 | 5.04e+13 | 3.94e+13 | 3.15e+13 | 2.45e+13 | 1.85e+13 | 8.74e+12 |
| | Si BSF/R | | | | | |
| 926 | 3.87e+13 | 2.31e+13 | 1.38e+13 | 9.46e+12 | 7.44e+12 | 5.24e+12 |
| 7408 | 7.83e+16 | 2.68e+16 | 6.15e+15 | 1.80e+15 | 6.87e+14 | 1.44e+14 |
| 20372 | 5.75e+13 | 4.42e+13 | 3.52e+13 | 2.73e+13 | 2.06e+13 | 9.71e+12 |

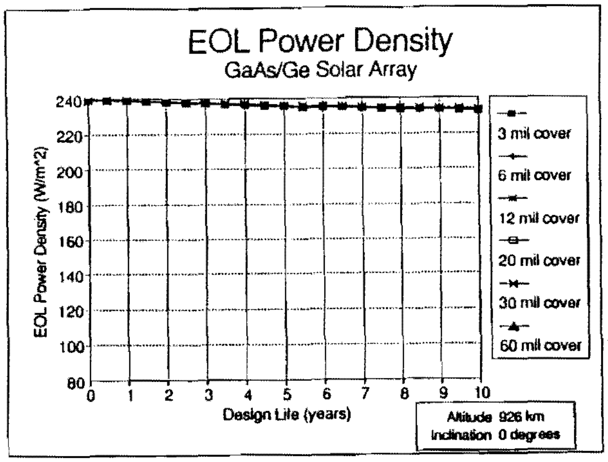


Figure 1

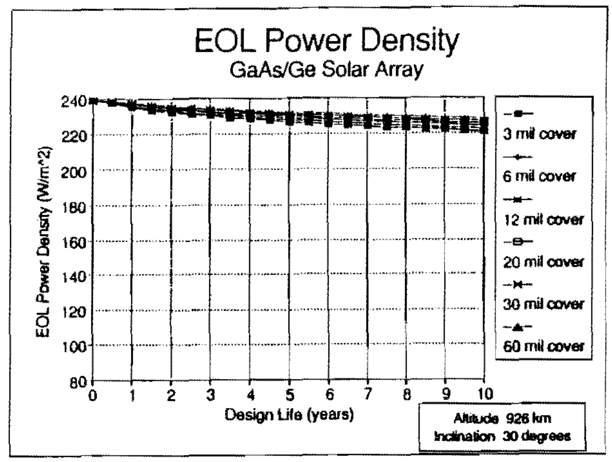


Figure 2

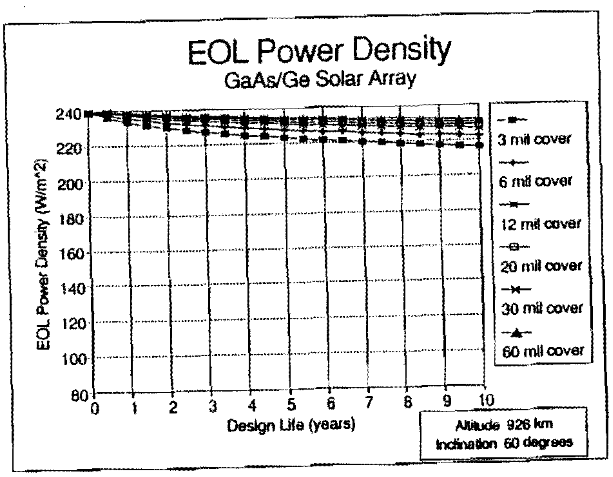


Figure 3

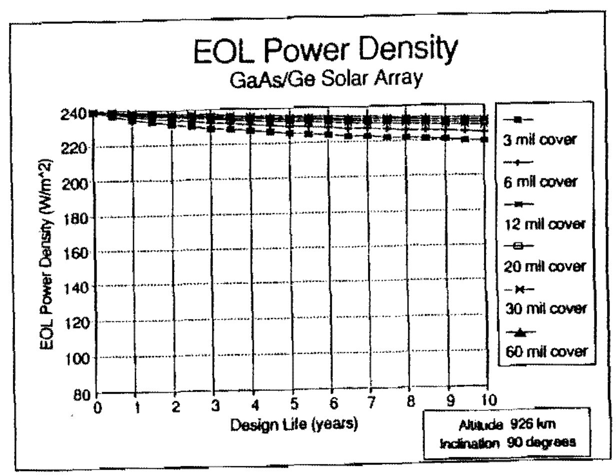


Figure 4

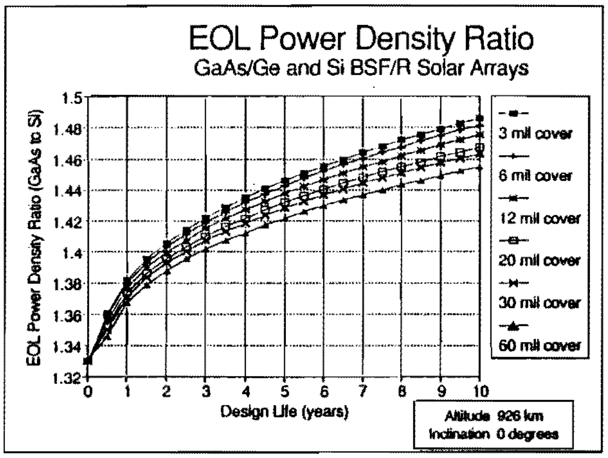


Figure 5

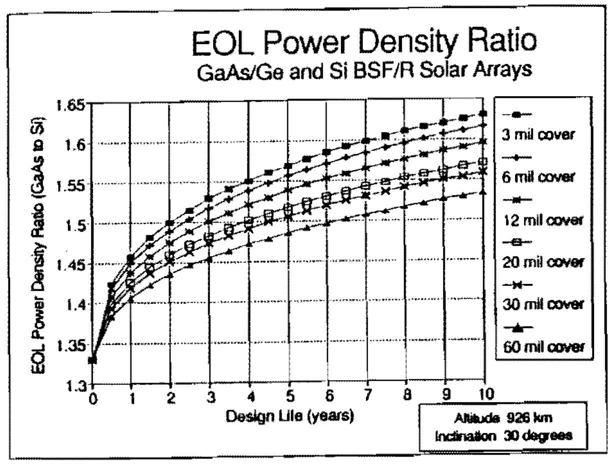


Figure 6

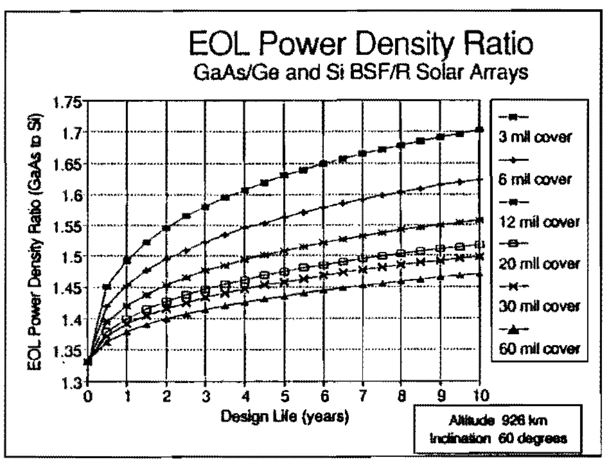


Figure 7

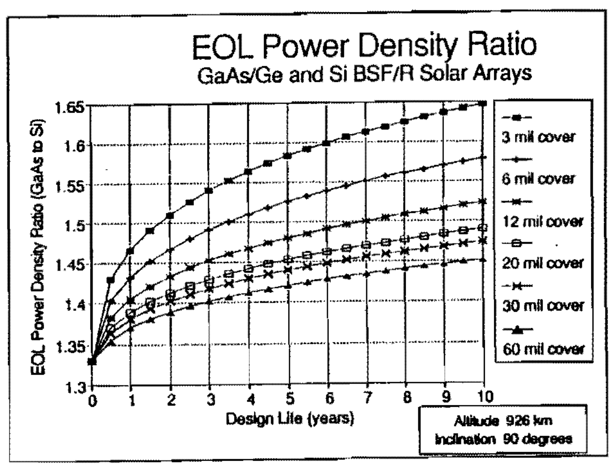


Figure 8

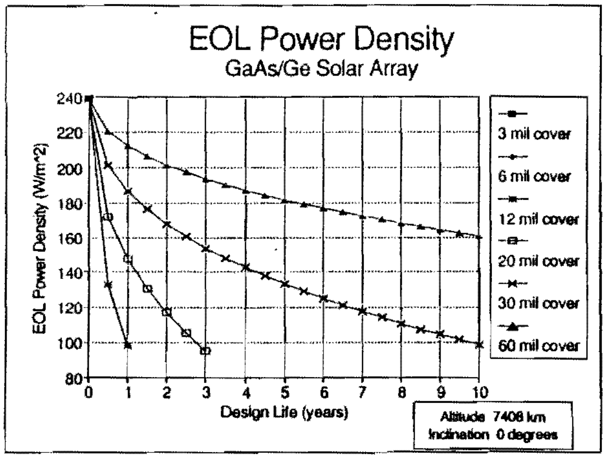


Figure 9

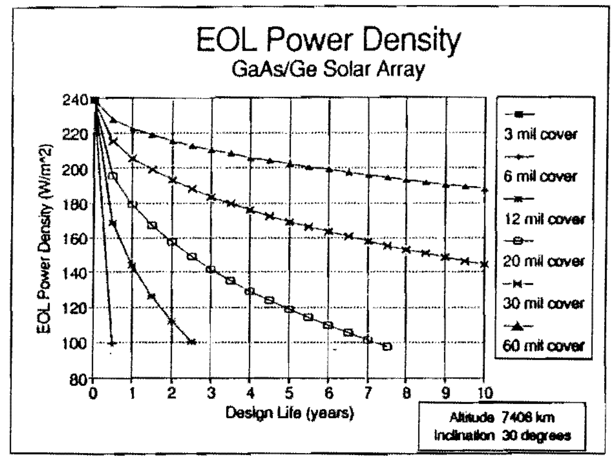


Figure 10

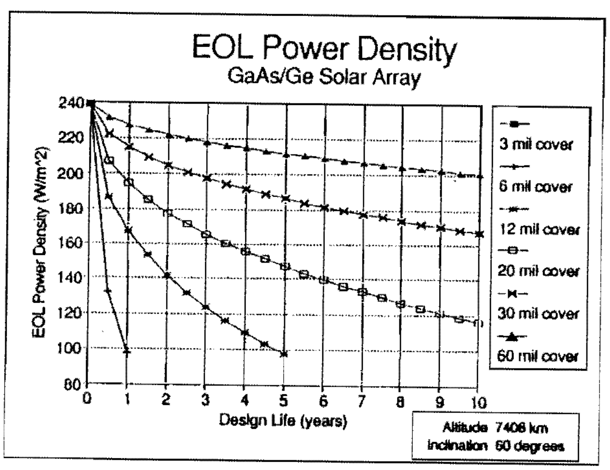


Figure 11

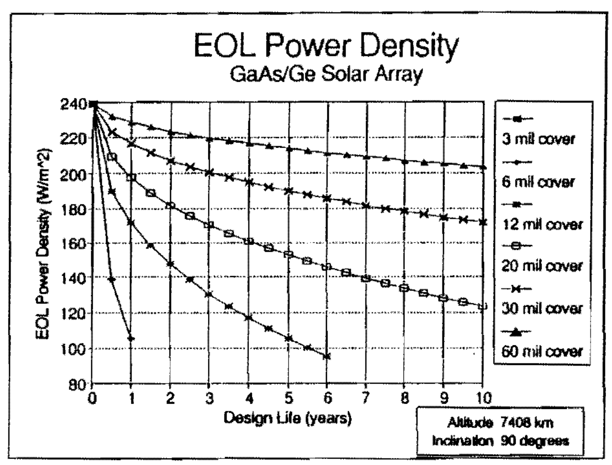


Figure 12

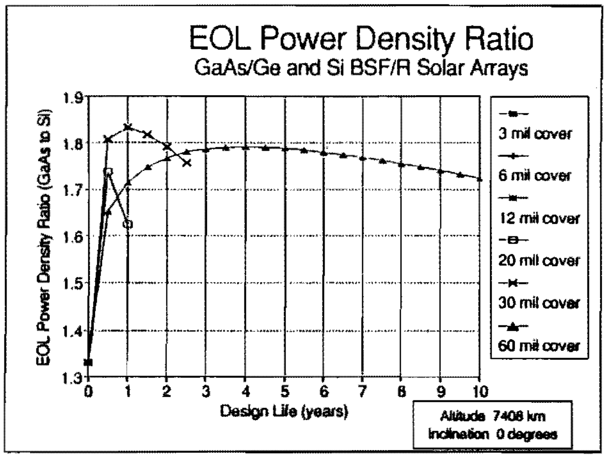


Figure 13

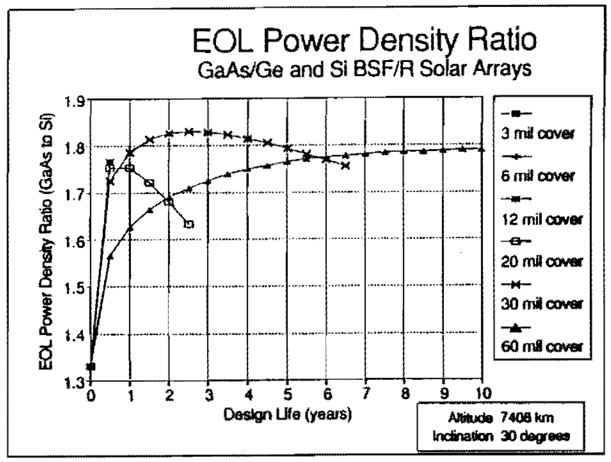


Figure 14

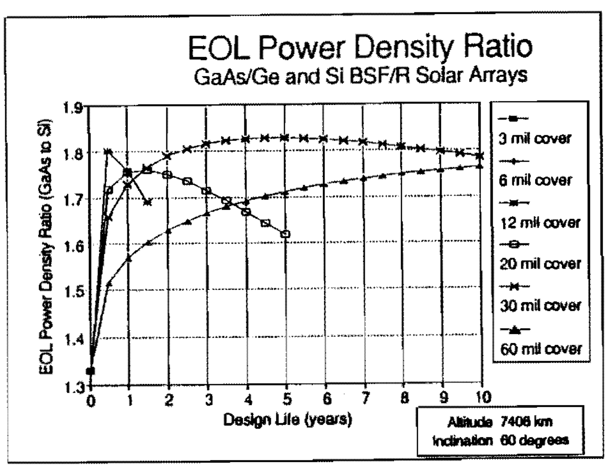


Figure 15

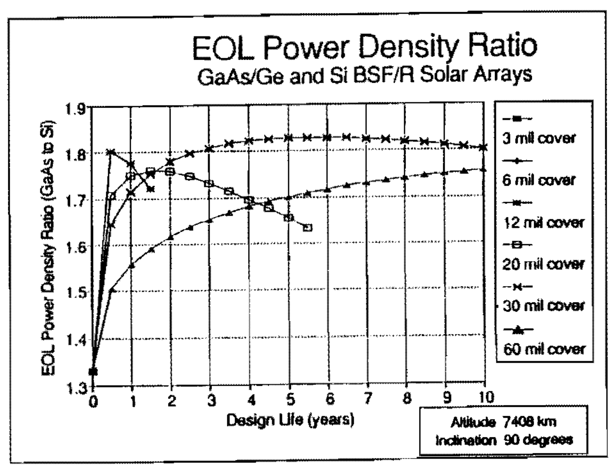


Figure 16

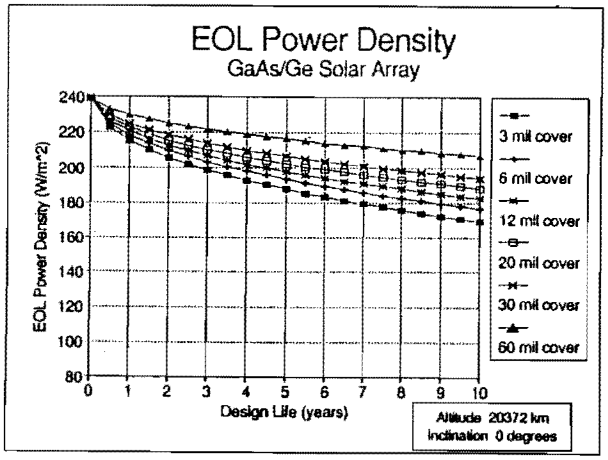


Figure 17

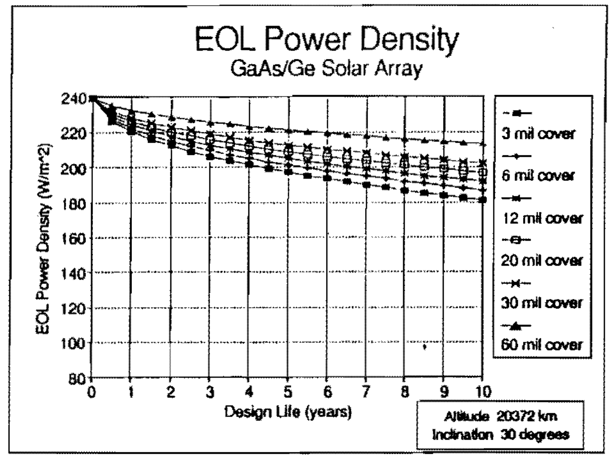


Figure 18

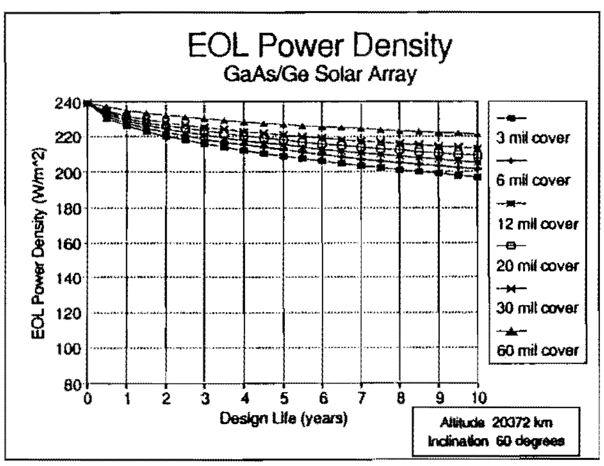


Figure 19

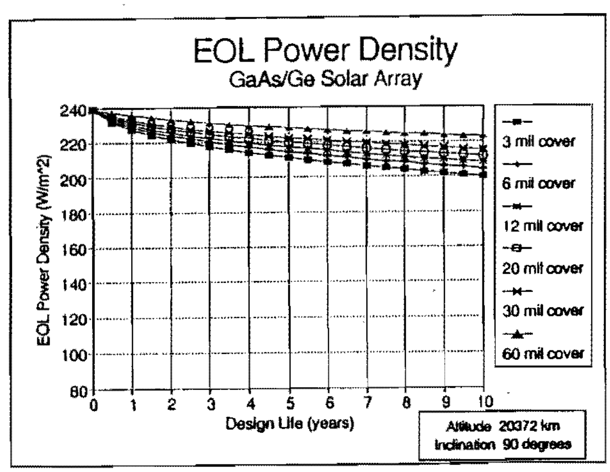


Figure 20

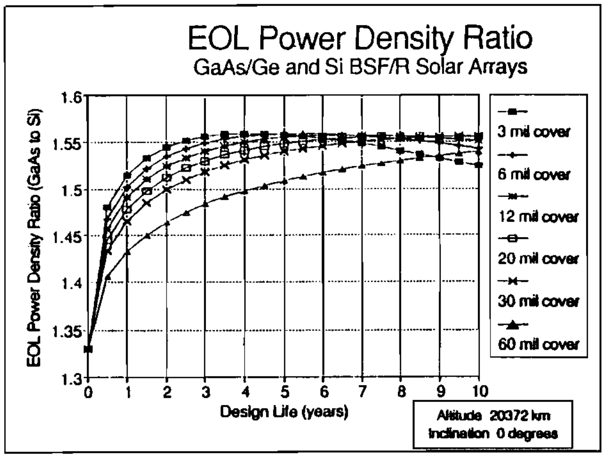


Figure 21

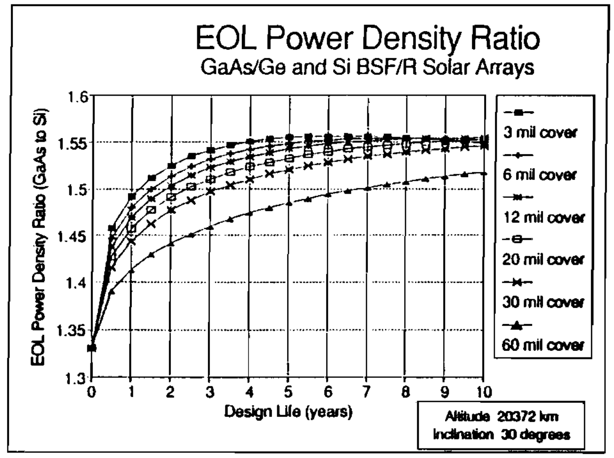


Figure 22

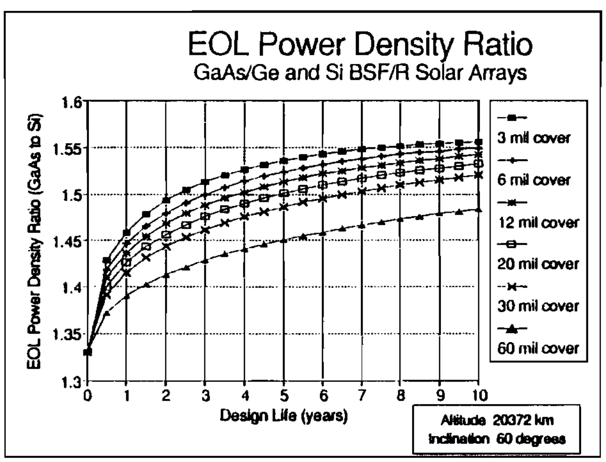


Figure 23

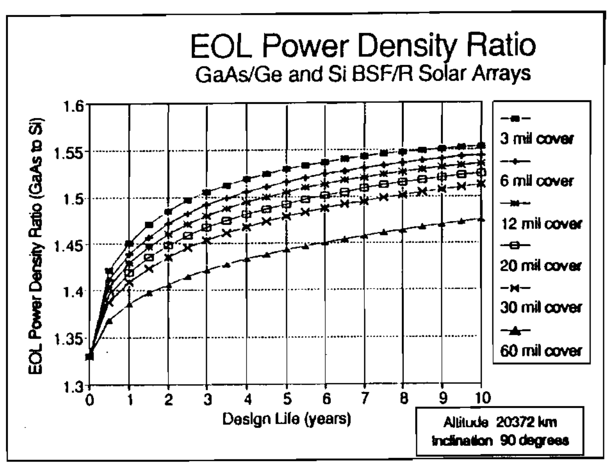


Figure 24

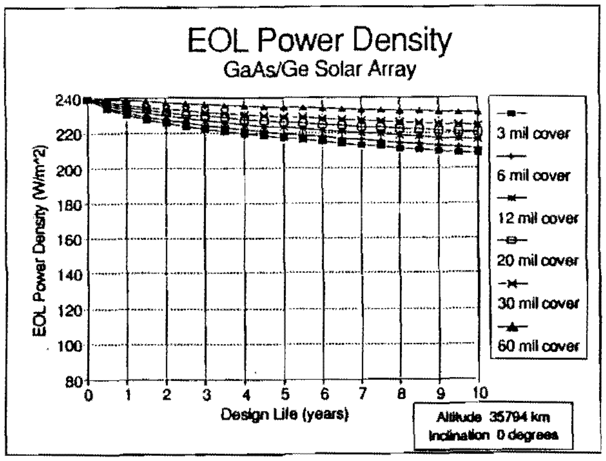


Figure 25

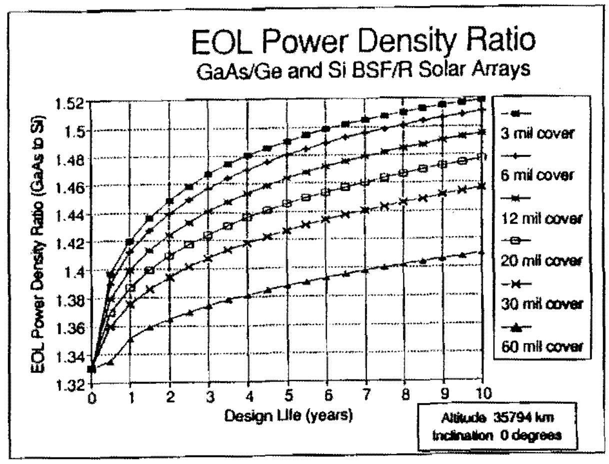


Figure 26